Self-consistent solution of Dyson's equation up to second order for open-shell atomic systems

K. Peirs,[a] D. Van Neck,[b] and M. Waroquier
Laboratory of Theoretical Physics, Ghent University, Proeftuinstraat 86, B-9000 Gent, Belgium

(Received 5 November 2001; accepted 11 June 2002)

Green's function techniques are powerful tools for studying interacting many-fermion systems in a structural and diagrammatical way. The central equation in this method is the Dyson equation which determines, through an approximation for the self-energy, the Green's function of the system. In a previous paper [J. Chem. Phys. **115**, 15 (2001)] a self-consistent solution scheme of the Dyson equation up to second order in the interaction, the Dyson(2) scheme, has been presented for closed-shell atoms. In this context, self-consistency means that the electron propagators appearing in a conserving approximation for the self-energy are the same as the solutions of the Dyson equation, i.e., they are fully dressed. In the present paper this scheme is extended to open-shell atoms. The extension is not trivial, due to the loss of spherical symmetry as a result of the partially occupied shells, but can be simplified by applying an appropriate angular averaging procedure. The scheme is validated by studying the second-row atomic systems B, C, N, O, and F. Results for the total binding energy, ionization energy and single-particle levels are discussed in detail and compared with other computational tools and with experiment. In open-valence-shell atoms a new quantity—the electron affinity—appears which was not relevant in closed-shell atoms. The electron affinities are very sensitive to the treatment of electron correlations, and their theoretical estimate is a stringent test for the adequacy of the applied scheme. The theoretical predictions are in good agreement with experiment. Also, the Dyson(2) scheme confirms the nonexistence of a stable negative ion of N. The overall effect of the self-consistent Dyson(2) scheme with regard to the Dyson(1) (i.e., Hartree–Fock) concept, is a systematic shift of all quantities, bringing them closer to the experimental values. The second-order effects turn out to be indispensable for a reasonable reproduction of the electron affinity.
[DOI: 10.1063/1.1497682]

I. INTRODUCTION

Computational schemes such as the Hartree–Fock and Density Functional Theory have become quite popular in the study of atomic and molecular systems over the years. These methods combine the advantage of computational speed with accuracy, allowing to tackle systems ranging from atoms to clusters of molecules. Nowadays, the effect of electron correlations remains one of the intriguing issues in scientific research and is the subject of several studies based on various computational tools. Density Functional Theory is capable of incorporating correlations in the calculations by the use of an additional degree of freedom: the exchange-correlation functional. However, no detailed picture of the nature of the correlations embedded in the functional is available. The quest to identify which correlations are dominant in atomic and molecular systems is stimulated by modern computer technology that makes the study of electron correlations via advanced first-principle calculations feasible.

One of these first-principle methods is the Green's function formalism. Reviews on how this theory is applied in quantum chemistry are given in several works (see, e.g., Refs. 1–7). This theory describes a many-body system by means of a single-particle (s.p.) propagator which carries all correlations resulting from the interaction with the other electrons in the atom or the molecule. The inclusion of medium effects in the construction of this so-called ''dressed'' electron propagator makes it an interesting and instructive tool to calculate in a most thorough way all ground-state properties of the electronic system, such as total binding energies, ionization energies, energy levels, occupation numbers, electron charge densities, etc. As a result of the amount of information included in the electron propagator many efforts have been invoked to solve Dyson's equation. While early attempts (e.g., Refs. 8–10) had to reduce the numerical efforts substantially, present computer technology allows a more advanced approach. Nevertheless, it is obvious that an exact solution scheme is excluded, since it would require the solution of a fully interacting many-particle problem.

The insertion of correlations in the electron propagator is ensured by the introduction of an energy-dependent potential: the so-called self-energy $[\Sigma(E)]$. It is related to the Green's function $[G(E)]$ by Dyson's equation,

$$[G(E)]=[G^0(E)]+[G^0(E)][\Sigma(E)][G(E)], \tag{1}$$

where $[G^0(E)]$ is the Green's function of the noninteracting system. The self-energy, in general a complex and nonlocal

[a]Author to whom correspondence should be addressed. Electronic mail: karel.peirs@rug.ac.be
[b]Electronic mail: dimitri.vanneck@rug.ac.be

operator, can be expanded order by order in the interaction, and contains all effects of the electron–electron interactions.

In the self-consistent formulation of Green's function theory, which we apply in the present work, the electron propagators in the expansion of the self-energy must be identical to the solution of the Dyson equation. Going beyond first order, this requires in particular that the popagators used in the evaluation of the self-energy have a nontrivial pole structure, much more complicated than the single-pole structure of the Hartree–Fock propagator.

The scheme offers a lot of opportunities to insert higher-order diagrams and infinite classes of diagrams, which may not be involved in standard perturbation techniques. The first-order approximation to Dyson's equation leads to the Hartree–Fock scheme. The corresponding Green's function can be used to calculate the Hartree–Fock values of all observables of the system. This first-order approach constructs the mean field in which the electrons move but ignores other electron correlation effects. To incorporate these effects in the s.p. propagator, insertion of higher-order diagrams (at least of second order) in the self-energy is prerequisite.

In a previous paper,[1] we addressed the problem of solving the Dyson equation self-consistently up to second order for closed-shell atoms. The topic of the current paper is to extend this method to open-shell atoms such that it covers atoms like C and O. Our algorithm has two major advantages. First, the self-consistency requirement, though it increases the computational cost considerably, ensures that basic conservation laws are fulfilled (e.g., number of particles). Second, the whole procedure is performed essentially without basis set limitations. The first-order Dyson equation is solved exactly in coordinate space, i.e., on a radial grid. To treat the continuum states in a feasible way, a discretization scheme is proposed, that necessarily leads to the introduction of a basis set. However, this basis set is truncated in such a way that second-order results for, e.g., the first ionization energy are unaffected by the truncation. Using this basis set (which is complete for all practical purposes), Dyson's equation is solved up to second order in a self-consistent way.

One of the main problems to overcome is the huge increase of the number of poles of the Green's function after some iterations. As in Ref. 1, we adopt the BAGEL (BAsis Generated by the Lanczos algorithm, see Refs. 11–15) approach to cope with this phenomenon. This algorithm provides a representation of the s.p. Green's function in terms of a few characteristic poles, chosen in such a way as to reproduce the lowest order moments of the exact distribution.

The open-shell systems selected in this paper are atoms of the second row of the periodic system: B, C, N, O, and F. In these cases a nonrelativistic approach is still acceptable but, contrary to the closed-shell atoms, the spins and angular momenta can couple to nonzero orbital angular momentum L, spin S, and total angular momentum J. In this work we give preference to using an uncoupled representation, because in this way the formalism as developed for the closed-shell case remains essentially unchanged, after performing a suitable angular average.

We did not take into account screening effects higher than second order generated by ring or ladder diagrams in the self-energy. These effects can be incorporated in the self-consistent scheme but complicate the proposed algorithm substantially and are at the present stage out of the scope of this work.

An extensive comparative study is presented with calculations at a high perturbative level and with other computational schemes (Hartree–Fock and Density Functional Theory methods). Sufficient experimental and computational data are available for all atoms under study to present a valuable discussion of the various theoretical results. In particular, special attention is paid to the reproduction of the total binding energy and ionization energies. These properties were also studied in Ref. 1 in case of closed-shell atoms. Since an open-shell atom is more likely to bind an additional electron, another interesting quantity, the electron affinity, enters into the discussion. It is well known that this quantity is difficult to reproduce due to the necessity of incorporating higher-order electron correlations beyond mean-field. Therefore, the electron affinity provides a stringent test for our scheme and it is demonstrated that the Dyson second-order scheme improves the HF results in a very substantial manner.

The outline of this paper is as follows. In Sec. II the numerical scheme is discussed and the changes compared to the closed-shell case in Ref. 1 are highlighted. In Sec. IV, we present our results and give special attention to a comparative analysis between the various schemes and experiment. Finally, a summary and some conclusions are formulated in Sec. V.

II. FORMALISM AND NUMERICAL SCHEME

In this section, we give a short overview of the algorithm to solve Dyson's equation self-consistently up to second order, and point out the extensions that are needed in open-shell systems. A more thorough discussion of the theoretical framework used in the present Dyson(2) scheme can be found in Ref. 1. Atomic units are used throughout the paper.

A. Mean-field procedure and angular averaging

First we address the impact of the open-shell features on the single-particle basis. In Ref. 1 a series of spin-saturated closed-shell atoms was treated nonrelativistically and without spin–orbit interaction. Using a spherical basis set with quantum numbers $\alpha=(n_a,l_a,m_{l_a},m_{s_a})$, only the principal and orbital angular momentum quantum numbers (n_a,l_a) differentiate the radial wave functions, and the orbitals show a degeneracy of $2(2l_a+1)$ in the values (m_{l_a},m_{s_a}) for the projection of orbital angular momentum and spin.

The extension presented here deals with the atoms B, C, N, O, and F, open-shell atoms having a partially filled $2p$ shell. If the angular and spin part of the spherical single-particle basis is retained,

$$\phi_\alpha(\mathbf{r})=\frac{1}{r}\varphi_\alpha(r)Y_{l_a m_{l_a}}(\Omega)\chi_{m_{s_a}}(\sigma), \tag{2}$$

the Hartree–Fock equations $(-\boldsymbol{\nabla}^2/2-Z/r-\epsilon_\alpha+\hat{V}_{\mathrm{HF}})\phi_\alpha(\mathbf{r})=0$, after integrating out the angular and spin dependence, become

$$\left(-\frac{1}{2}\left[\frac{d^2}{dr^2}-\frac{l_a(l_a+1)}{r^2}\right]-\frac{Z}{r}-\epsilon_\alpha\right)\varphi_\alpha(r)$$
$$+\sum_{\beta(\mathrm{occ.})}\int dr' D_{\alpha\beta}(r,r')\varphi_\beta(r')^2\varphi_\alpha(r)$$
$$-\sum_{\beta(\mathrm{occ.})}\int dr' E_{\alpha\beta}(r,r')\varphi_\beta(r')\varphi_\alpha(r')\varphi_\beta(r)=0. \quad (3)$$

The summation over β includes only the s.p. states that are occupied in the Hartree–Fock ground state. The direct and exchange contributions to the HF potential read

$$D_{\alpha\beta}(r,r')=\sum_{LM}\frac{r_<^L}{r_>^{L+1}}\frac{4\pi}{2L+1}\langle l_b m_{l_b}|Y_{LM}|l_b m_{l_b}\rangle \times\langle l_a m_{l_a}|Y_{LM}^*|l_a m_{l_a}\rangle,$$

$$E_{\alpha\beta}(r,r')=\sum_{LM}\frac{r_<^L}{r_>^{L+1}}\frac{4\pi}{2L+1}\langle l_b m_{l_b}|Y_{LM}|l_a m_{l_a}\rangle \times\langle l_a m_{l_a}|Y_{LM}^*|l_b m_{l_b}\rangle, \quad (4)$$

where

$$\langle l_b m_{l_b}|Y_{LM}|l_a m_{l_a}\rangle=\int d\Omega Y^*_{l_b m_{l_b}}(\Omega)Y_{LM}(\Omega)Y_{l_a m_{l_a}}(\Omega). \quad (5)$$

The HF equations (3) depend on the choice of the occupied $2p$ orbitals (except for the N atoms where we assume full occupation of the $2p$ orbital of one spin type). As a consequence, the radial wave functions and s.p. energies depend on (m_{l_a},m_{s_a}) as well as on (n_a,l_a). Keeping track of the full set of spherical quantum numbers would become unmanageable in the subsequent self-consistent Green's function calculation, and we therefore introduce, in case of B, C, O, and F atoms, the following angular averaging procedure. For the N atoms no angular averaging is needed.

The $l\neq 1$ orbitals are all fully occupied or completely empty. For these levels we perform a spherical averaging by summing in Eq. (5) over all substates m_l and dividing by the degeneracy $2l+1$. These orbitals are described by radial wave functions $\varphi_a(r)$ characterized by the quantum numbers $a=(n_a,l_a,m_{s_a})$, independent of m_{l_a}.

For the $l=1$ orbitals the angular averaging is somewhat more complicated due to the presence of a partially filled $2p$ spin orbital, and should be performed in such a way as to prevent self-interaction in the HF mean field for the $2p$ occupied states. The basic idea is to reduce the number of radial wave functions corresponding with different m_l quantum numbers, and limit the representation of the $l=1$ space to two types of radial wave functions, one associated with the occupied $2p$ subspace (denoted $\kappa=1$), and one associated with the unoccupied $2p$ subspace (denoted $\kappa=0$). In this way the $l=1$ spin orbitals are characterized by quantum numbers $a=(n_a,l_a=1,m_{s_a},\kappa_a)$, independent of m_{l_a}. The corresponding degeneracy d_a depends on the partial filling n_p of the $2p$ spin orbital with one or two electrons: $n_p=1$ for the B and O atoms, and $n_p=2$ for the C and F atoms. For $l_a=1$ we thus have $d_a=n_p$ for $\kappa_a=1$ and $d_a=3-n_p$ for $\kappa_a=0$. For clarity the scheme is visualized in Fig. 1.

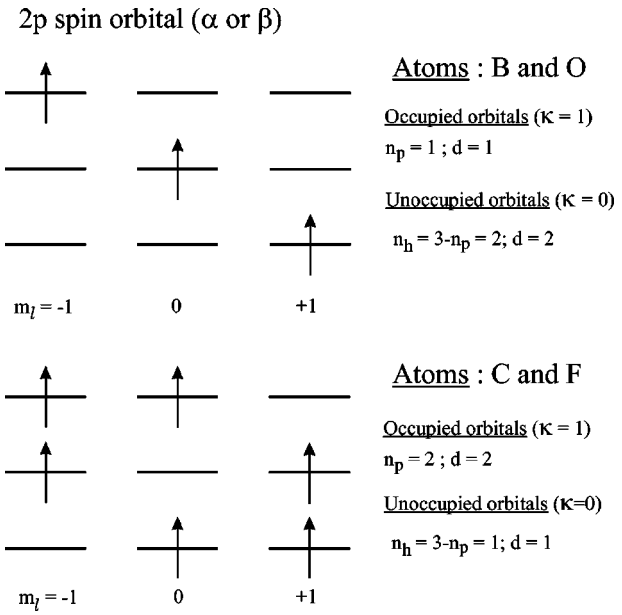

FIG. 1. Partially filled $2p$ spin orbital in the open-shell atoms B, C, O, and F. n_p denotes the number of electrons in the partially filled spin orbital, while d stands for the degeneracy of the orbital characterized by quantum numbers n,l,m_s,κ.

The procedure described above leads to the following averaged HF potential:

$$\overline{D}_{ab}(r,r')=\frac{1}{(2l_a+1)(2l_b+1)}\sum_{m_{l_a}m_{l_b}}D_{\alpha\beta}(r,r') \quad (6)$$

for $l_a\neq 1$ and/or $l_b\neq 1$,

$$\overline{D}_{ab}(r,r')=\frac{1}{3}\sum_{m_{l_a}m_{l_b}}D_{\alpha\beta}(r,r')\delta_{m_{l_a}m_{l_b}} \quad (7)$$

for $l_a=l_b=1$ and $d_a=d_b=1$,

$$\overline{D}_{ab}(r,r')=\frac{1}{12}\sum_{m_{l_a}m_{l_b}}D_{\alpha\beta}(r,r')(1+\delta_{m_{l_a}m_{l_b}}) \quad (8)$$

for $l_a=l_b=1$ and $d_a=d_b=2$, and

$$\overline{D}_{ab}(r,r')=\frac{1}{6}\sum_{m_{l_a}m_{l_b}}D_{\alpha\beta}(r,r')(1-\delta_{m_{l_a}m_{l_b}}) \quad (9)$$

for $l_a=l_b=1$, $d_a=1$ and $d_b=2$ (or $d_a=2$ and $d_b=1$). The same expressions hold for the exchange part $\overline{E}_{ab}(r,r')$ of the HF potential.

In a more compact notation, which will be used in the remainder of the paper, the angular averaged HF potential is rewritten as,

$$\overline{D}_{ab}(r,r')=\frac{1}{3}\sum_\mu\frac{1}{d_a d_b}\sum_{m_{l_a}m_{l_b}}w_{\alpha\mu}w_{\beta\mu}D_{\alpha\beta}(r,r'),$$
$$\overline{E}_{ab}(r,r')=\frac{1}{3}\sum_\mu\frac{1}{d_a d_b}\sum_{m_{l_a}m_{l_b}}w_{\alpha\mu}w_{\beta\mu}E_{\alpha\beta}(r,r'), \quad (10)$$

TABLE I. Values in atomic units for the parameters R_l and C_l of the parabolic potential [see Eq. (13)], and number of radial wave functions retained in the discretization of the continuum. Between square brackets, the spectroscopic notation of the ground state of the atom is given.

		B $[^2P_{1/2}]$	C $[^3P_0]$	N $[^4S_{3/2}]$	O $[^3P_2]$	F $[^2P_{3/2}]$
$l=0$	R_l; C_l	7.7; 5.0	6.0; 5.0	5.0; 5.0	3.8; 5.0	3.5; 5.0
	occ.	$1s-2s$	$1s-2s$	$1s-2s$	$1s-2s$	$1s-2s$
	virt.	$3s-16s$	$3s-15s$	$3s-19s$	$3s-15s$	$3s-16s$
$l=1$	R_l; C_l	7.7; 5.0	6.0; 5.0	4.3; 5.0	3.9; 5.0	3.5; 5.0
	occ.	$2p$	$2p$	$2p$	$2p$	$2p$
	virt.	$3p-16p$	$3p-17p$	$3p-18p$	$3p-17p$	$3p-17p$
$l=2$	R_l; C_l	3.9; 5.0	2.0; 5.0	0.0; 5.0	0.0; 5.0	0.0; 5.0
	virt.	$3d-13d$	$3d-12d$	$3d-14d$	$3d-11d$	$3d-12d$
$l=3$	R_l; C_l	2.8; 5.0	1.5; 5.0	0.0; 5.0	0.0; 5.0	0.0; 5.0
	virt.	$4f-12f$	$4f-8f$	$4f-12f$	$4f-10f$	$4f-12f$
$l=4$	R_l; C_l	2.1; 5.0	1.0; 5.0	0.0; 5.0	0.0; 5.0	0.0; 5.0
	virt.	$5g-11g$	$5g-7g$	$5g-10g$	$5g-10g$	$5g-12g$
$l=5$	R_l; C_l	1.5; 5.0	0.5; 5.0	0.0; 5.0	0.0; 5.0	0.0; 5.0
	virt.	$6h-11h$	$6h-7h$	$6h-8h$	$6h-8h$	$6h-12h$
$l=6$	R_l; C_l			0.0; 5.0	0.0; 5.0	0.0; 5.0
	virt.			$7i-8i$	$7i$	$7i-10i$
$l=7$	R_l; C_l					0.0; 5.0
	virt.					$8j-9j$

where the summation over m_{l_a} and m_{l_b} is restricted by the $w_{\alpha\mu}$ coefficients according to

$$\left\{ \begin{array}{lll} l_a \neq 1 & & : w_{\alpha\mu}=1 \\ l_a=1, & d_a=2 & : w_{\alpha\mu}=1-\delta_{m_{l_a}\mu} \\ l_a=1, & d_a=1 & : w_{\alpha\mu}=\delta_{m_{l_a}\mu}. \end{array} \right\}. \tag{11}$$

In Eq. (10) the factor 1/3 and summation over $\mu=-1,0,1$ correspond to an averaging over the choice of occupied m_l values in the $2p$ spin orbital. The coefficients $w_{\alpha\mu}$ in Eq. (11) then automatically select the correct m_l values for each choice of μ.

The final HF equations in radial space (for occupied as well as unoccupied states) read

$$\left(-\frac{1}{2}\left[\frac{d^2}{dr^2} - \frac{l_a(l_a+1)}{r^2} \right] - \frac{Z}{r} - \epsilon_a \right) \varphi_a(r) + \sum_{b(\text{occ.})} d_b \int dr' \overline{D}_{ab}(r,r') \varphi_b(r')^2 \varphi_a(r) - \sum_{b(\text{occ.})} d_b \int dr' \overline{E}_{ab}(r,r') \varphi_b(r') \varphi_a(r') \varphi_b(r) = 0. \tag{12}$$

In summary, we allow different spin orbitals for the two spin species. The angular averaging procedure results, for $m_s=\pm\frac{1}{2}$, in a single HF Hamiltonian for each $l\neq 1$, and two HF Hamiltonians, corresponding to $\kappa=0$ and $\kappa=1$, in the $l=1$ case. The construction of a complete and orthonormal set of s.p. states is then straightforward. Compared to the closed-shell case in Ref. 1, the number of s.p. states is roughly doubled, with a corresponding increase in the numerical effort.

B. Dyson(1) calculation and construction of virtual orbitals

In this subsection we discuss the numerical procedure to construct the set of s.p. states which is used subsequently for the second-order calculation. The construction is such that it approaches an almost exact treatment in coordinate space.

The HF equations (12) are first solved in coordinate space on a radial grid, in order to avoid the inaccuracies inherent to the use of a finite basis set (e.g., of Gauss-type orbitals). This yields the occupied (hole) states and the HF mean field. The higher-order diagrams in the self-energy of the Dyson(2) scheme also involve intermediary propagators for the virtual or unoccupied (particle) states. Since an exact treatment of the continuum part of the HF Hamiltonian becomes prohibitive, the continuum states are discretized as follows.

We add to the HF potential a parabolic potential wall, at a relatively large distance from the atomic center [we denote the step function by $\theta(x)$],

$$U_l(r)=C_l\theta(r-R_l)(r-R_l)^2. \tag{13}$$

It turns out to be advantageous to introduce a parabolic wall for each group of orbitals with the same orbital angular momentum l. The values of the two parameters characterizing the parabolic potential are always chosen such that they do not effect the HF results for all occupied states (in other words that they coincide to high accuracy with the exact HF results without the wall). The precise method for choosing the wall parameters also involves an optimum speed of convergence of the second-order results in terms of the number of virtual orbitals, and is explained in Sec. III. In Table I the used values of the parameters C_l and R_l are listed.

Both occupied and unoccupied orbitals (which are also bound in this scheme) are constructed in coordinate space, as eigenfunctions of the exact HF Hamiltonian modified *with* the addition of the parabolic potential. The eigenfunctions

form a complete and orthonormal set, but a truncation of the basis set is needed for practical purposes. However, the truncation is done in a controlled manner, which does not affect the final results. We also refer to Sec. III for a detailed discussion of this procedure. It turns out that about 100–200 orbitals are required to get sufficient convergence. The basis sets used in the calculations are listed in Table I as well.

At this point we have a discrete and finite basis set. The Dyson(1) calculation amounts to diagonalizing, within this basis set, the HF Hamiltonian matrix *without* the confining parabolic potential. Of course the s.p. energies of the hole states still correspond almost exactly to the coordinate space HF results. The discrete HF basis obtained in this way is then used as the starting point of the self-consistent Dyson(2) calculation.

C. Dyson(2) calculation

We will assume the s.p. propagator and the corresponding self-energy to be diagonal in the discrete HF basis obtained in the previous subsection. In the closed-shell case treated in Ref. 1, it was clear that nondiagonal contributions could only occur between s.p. states differing exclusively in their principal quantum number. For the present treatment of open-shell systems in the uncoupled representation a similar statement can be made using conservation of the projection of total angular momentum and spin. Note that the angular averaging scheme as introduced in Sec. II A is consistent with this.

In general the energy separation between orbitals with the same principal quantum number n is large enough to reduce intershell mixing, though this reasoning becomes questionable for the discretized continuum states. It should also be stressed that the assumption of diagonality in the principal quantum number is not strictly necessary, but serves to make the equations more tractable and to decrease the numerical effort. In future work we plan to study the effects of intershell mixing. The present results for, e.g., the electron affinity are in fairly good agreement with experiment, indicating that the effects are certainly not dominant.

Using the s.p. labels a as introduced in Sec. II A, the spectral representation of the Green's function can be written as a sum of simple poles,

$$G_a(E)=\sum_j \frac{S^f_{a,j}}{E-\epsilon^f_{a,j}+i\eta}+\sum_j \frac{S^b_{a,j}}{E-\epsilon^b_{a,j}-i\eta}. \tag{14}$$

The coefficients $S^f_{a,j}$ and $S^b_{a,j}$ in Eq. (14) are defined as

$$\begin{aligned} S^f_{a,j}&=|\langle j(A+1)_a|c^+_a|0(A)\rangle|^2,\\ S^b_{a,j}&=|\langle j(A-1)_a|c_a|0(A)\rangle|^2, \end{aligned} \tag{15}$$

and represent the spectroscopic factors for, respectively, the addition and removal of an electron in spin orbital a from the correlated A-electron ground state $|0(A)\rangle$. The summation index j is restricted to the $(A\pm1)$-electron states that can be reached from the ground state by adding or removing an electron in spin orbital a. The corresponding energies of these $(A\pm1)$-electron states are related to the $\epsilon^f_{a,j}$ and $\epsilon^b_{a,j}$ in Eq. (14) as

$$\begin{aligned} \epsilon^f_{a,j}&=\langle j(A+1)_a|H|j(A+1)_a\rangle-E_{0(A)},\\ \epsilon^b_{a,j}&=E_{0(A)}-\langle j(A-1)_a|H|j(A-1)_a\rangle. \end{aligned} \tag{16}$$

The spectroscopic factors are a measure of the fragmentation of spin orbital a over the states of the $(A\pm1)$ system due to correlations. In the HF approximation, the Green's function $G^{\mathrm{HF}}_a(E)$ has only one pole, corresponding to the HF energy ϵ^{HF}_a of spin orbital a, with the corresponding spectroscopic factor equal to unity. The resulting expression is

$$G^{\mathrm{HF}}_a(E)=\frac{\theta(\epsilon^{\mathrm{HF}}_a-\epsilon_F)}{E-\epsilon^{\mathrm{HF}}_a+i\eta}+\frac{\theta(\epsilon_F-\epsilon^{\mathrm{HF}}_a)}{E-\epsilon^{\mathrm{HF}}_a-i\eta}\ , \tag{17}$$

where ϵ_F is the Fermi energy of the system.

In a self-consistent formulation, the dressed propagators of Eq. (14) should be used to evaluate the electron self-energy. The contribution of second order in the interaction then reads

$$\Sigma^{(2)}_a(E)=\sum_{b,c,d}\frac{F_{ab,cd}}{2d_a}\left\{\sum_{j,k,l}\frac{S^f_{c,j}S^f_{d,k}S^b_{b,l}}{E-(\epsilon^f_{c,j}+\epsilon^f_{d,k}-\epsilon^b_{b,l})+i\eta}+\sum_{j,k,l}\frac{S^b_{c,j}S^b_{d,k}S^f_{b,l}}{E-(\epsilon^b_{c,j}+\epsilon^b_{d,k}-\epsilon^f_{b,l})-i\eta}\right\}. \tag{18}$$

The interaction coefficients $F_{ab,cd}$ in Eq. (18) are angular averaged in case of a partially filled $2p$-shell, consistently with the procedure used for the mean field in Eqs.(10)–(11). The general expression in terms of (antisymmetrized) matrix elements of the Coulomb interaction V reads

$$F_{ab,cd}=\frac{1}{3}\sum_{\mu}\sum_{m_{l_a},m_{l_b},m_{l_c},m_{l_d}} w_{\mu m_{l_a}}w_{\mu m_{l_b}}w_{\mu m_{l_c}}w_{\mu m_{l_d}} \times|\langle(am_{l_a})(bm_{l_b})|V|(cm_{l_c})(dm_{l_d})\rangle_{as}|^2, \tag{19}$$

where the summation over $\mu=-1,0,1$ represents the averaging over the occupied m_l values in the $2p$ shell.

The self-consistent solution is then found by the following iteration process:

$$G^{[n+1]}_a(E)=\frac{1}{E-\epsilon^{\mathrm{HF}[n]}_a-\Sigma^{(2)[n]}_a(E)} \tag{20}$$

$$=\sum_j\frac{S^{f[n+1]}_{a,j}}{E-\epsilon^{f[n+1]}_{a,j}+i\eta}+\sum_j\frac{S^{b[n+1]}_{a,j}}{E-\epsilon^{b[n+1]}_{a,j}-i\eta}. \tag{21}$$

The HF propagator is used as the starting point $(n=0)$ of the iterative scheme.

The second-order self-energy in the nth iteration, $\Sigma^{(2)[n]}_a(E)$, is constructed with the nth iteration propagator, i.e., Eq. (18) is evaluated with $S^{f[n]}_{a,j}$, $\epsilon^{f[n]}_{a,j}$, $S^{b[n]}_{a,j}$, and $\epsilon^{b[n]}_{a,j}$, representing the fragmented distribution of spectral strength in the nth iteration step. Also the first-order contribution $\Sigma^{(1)}$ to the self-energy must be evaluated with the dressed Green's function, resulting in HF-type energies which are updated in each iteration step as

$$\epsilon_a^{\mathrm{HF}[n]} = \langle a|H_0|a\rangle + \frac{1}{d_a}\frac{1}{3} \times \sum_{\mu} \sum_{c,m_{l_c},m_{l_a}} w_{\mu m_{l_a}} w_{\mu m_{l_c}} \langle \alpha\gamma|V|\alpha\gamma\rangle_{as} \sum_j S_{c,j}^{b\,[n]}, \tag{22}$$

where H_0 is the one-body part (kinetic energy and nuclear Coulomb field) of the Hamiltonian.

Note that during the iteration process of Eq. (20) the number of poles in the self-energy $\Sigma_a^{(2)[n]}(E)$ is roughly equal to the third power of the number of poles in the propagator $G_a^{[n]}(E)$, as can be seen from Eq. (18). This means that during each successive iteration the number of poles in the propagator is cubed. As in Ref. 1, the BAGEL scheme[11–15] is adopted to reduce the growing number of poles.

The basic idea of the BAGEL scheme consists of replacing the poles and residues in the self-energy by a smaller set of BAGEL poles, chosen so as to conserve some important properties of the original self-energy. The forward and backward parts of the self-energy in Eq. (18) can be written in a compact form as

$$\Sigma_a^{(2)}(E) = \sum_{J=1}^{D^f} \frac{\sigma_J^f}{E-\omega_J^f+i\eta} + \sum_{J=1}^{D^b} \frac{\sigma_J^b}{E-\omega_J^b-i\eta}. \tag{23}$$

The distribution of the large number D^f of residues and energies (σ_J^f, ω_J^f) is then replaced by the smaller BAGEL set $(\tilde{\sigma}_j^f, \tilde{\omega}_j^f)$, where $j=1,\ldots,M$. This BAGEL set is determined by the requirement that the lowest energy-weighted moments are equal for both distributions, i.e.,

$$\sum_{j=1}^{M} \tilde{\sigma}_j^f (\tilde{\omega}_j^f)^p = \sum_{J=1}^{D^f} \sigma_J^f (\omega_J^f)^p, \tag{24}$$

where $p=0,1,\ldots,2M-1$. A similar construction is used for the backward part of the self-energy.

In each iteration step we can now replace the complete self-energy by its BAGEL approximation using a fixed number of M poles in the forward and backward part. In this way the number of poles in the propagator remains the same during successive iterations.

For a sufficiently large number of BAGEL poles, this replacement has no influence on the distribution of spectroscopic strength near the Fermi energy, nor on the total binding energy. In the next section we discuss the convergence of the results with respect to the number of BAGEL poles. About 20 poles ($M=20$) are required to reach convergence, i.e., taking a larger number of poles has no significant effect on the binding energy, valence ionization energy or electron affinity.

The system of equations Eqs. (24) can be solved for the BAGEL energies and strengths using a variant of the Lanczos procedure.[11–14] The virtue of the BAGEL construction, where one demands reproduction of the lowest-order energy-weighted moments, lies in the fast convergence of the solutions of the Dyson equation for energies near the Fermi-energy, using the BAGEL approximations for the self-energy in terms of a small number of poles. This is directly related to the property of the numerical Lanczos method of fast convergence for the extremal eigenvalues of a symmetric matrix.[16] Moreover, the total binding energy in the Dyson(2) scheme can be calculated (see Ref. 1) using the Galitskii–Migdal expression,

$$E_{gs}(A) = \frac{1}{2}\sum_{aj} (\langle a|H_0|a\rangle + \epsilon_{a,j}^b) S_{a,j}^b, \tag{25}$$

and is seen to depend only on the zeroth and first energy-weighted moment of the backward distribution of spectroscopic strength. The moment reproduction for the self-energy then ensures a fast convergence also for the total binding energy, as seen from the results in the next section.

TABLE II. Carbon first ionization energy (atomic units). Results obtained using the second-order self-energy in the first iteration (see text). Only *s* and *p* orbitals were considered. The parameters of the parabolic potential are $C_l=5$, and $R_l=3$ (top), $R_l=6$ (middle), $R_l=10$ (bottom). N_s: number of *s*-orbitals, increasing with row number. N_p: number of *p*-orbitals, increasing with column number.

$R_l=3$	$N_p=10$	15	20	25
$N_s=10$	0.3878	0.3921	0.3936	0.3960
15	0.3894	0.3937	0.3952	0.3964
20	0.3898	0.3941	0.3956	0.3966
25	0.3962	0.3965	0.3966	0.3966
$R_l=6$	$N_p=10$	15	20	25
$N_s=10$	0.3963	0.3964	0.3964	0.3964
15	0.3964	0.3965	0.3966	0.3966
20	0.3964	0.3966	0.3966	0.3966
25	0.3964	0.3966	0.3966	0.3966
$R_l=10$	$N_p=10$	15	20	25
$N_s=10$	0.3960	0.3961	0.3961	0.3961
15	0.3962	0.3964	0.3964	0.3964
20	0.3962	0.3965	0.3965	0.3966
25	0.3962	0.3965	0.3966	0.3966

III. CHOICE OF BASIS SET AND PARAMETERS

In this section we illustrate how several parameters that enter the calculation, such as the confining potential, the number of virtual orbitals, and the number of BAGEL poles, were chosen. We use the calculation for the carbon atom as an example.

The number of virtual orbitals was determined by considering the ionization energy $\mathcal{I}_1$ in the first iteration, i.e., using the HF propagators to evaluate the self-energy and solving the corresponding Dyson equation for the highest occupied level. All two-hole/one-particle and two-particle/one-hole intermediate states are taken into account in the second-order self-energy; the BAGEL approximation was not yet used at this level. Table II contains the ionization energy for a test calculation where only *s* and *p*-orbitals are considered, for an increasing number of virtual orbitals, and for three quite different parabolic potentials [see Eq.(13)].

The value of $C_l=5$ is taken constant, but the parameter R_l, which determines the position of the wall, is taken as $R_l=3$, $R_l=6$, and $R_l=10$, respectively.

It is clear from Table II that the ionization energy converges to the same value for all choices of the parabolic potential, provided enough virtual orbitals are taken into account. However, the convergence is fastest using the parabolic potential with $R_l=6$. This is understood by realizing that for a small value of the wall distance R_l the confining potential distorts the HF potential and hence the bound orbitals . It then requires a large number of virtual orbitals to get back to the coordinate space HF wave functions and energies. On the other hand, for a very large value of R_l the level spacing of the virtual orbitals becomes quite small. In this case a large number of virtual orbitals are needed to provide a cut-off in energy which is sufficient to reach convergence for the second-order diagram. The same holds true if, instead of the position R_l, the curvature C_l of the parabolic potential is made very small. Stated differently, there exists an optimal value for the parameters of the confining potential, which allows an accurate discretization of the HF continuum in terms of a limited set of virtual orbitals, and leads to fast convergence of the second-order self-energy.

The parameter values of the confining potential which are listed in Table I were determined by a great number of test calculations like the one described above, involving first the l-values corresponding to the occupied HF states, and in a second stage the higher l-values. In all cases we checked convergence for the first ionization energy, up to 10^{-4} a.u. by gradually increasing the number of virtual orbitals. Then we determined the parameter R_l for which convergence was optimal in terms of the number of virtual orbitals. The value of C_l was kept fixed at $C_l=5$ a.u. which we found to be a reasonable value in all calculations. Note that inclusion of angular momenta with $l\geqslant 8$ did not affect the ionization energy $\mathcal{I}_1$ up to the required accuracy. This procedure resulted in the basis sets presented in Table I.

At this point we have converged results, in terms of the basis-set dimension, for the second-order diagram evaluated with HF propagators, i.e., the first iteration result in our iteration scheme towards the self-consistent solution. For the case of the carbon atom, e.g., we find a value of 0.4166 a.u. for the ionization energy $\mathcal{I}_1$. As mentioned in Sec. II, the self-energy is replaced by a BAGEL approximation in order to keep the number of poles under control. We next investigated the dependence of the first ionization energy, as a function of the number of BAGEL poles M, by solving the Dyson equation with the self-energy in the corresponding BAGEL approximation. For $M=10,15,20$ the result is, respectively, $\mathcal{I}_1=0.4171$, 0.4167, 0.4166. Note the convergence, with increasing number of poles, to the first-iteration result obtained without the BAGEL approximation. In our self-consistent calculations $M=20$ BAGEL poles are taken into account. This is sufficient to guarantee converged results for the ionization energy, electron affinity, and total binding energy. For carbon we checked this explicitely by performing fully self-consistent calculations with $M=10$ and $M=15$ poles, in addition to the standard $M=20$ poles. For the carbon binding energy (in atomic units) we find -37.790, -37.789, -37.789 for $M=10,15,20$ poles, respectively. This indicates the rapid convergence of the binding energy, which is essentially converged even at $M=10$. The results for the ionization energy, 0.417, 0.416, 0.415, behave similarly, whereas the results for the electron affinity, 0.040, 0.045, 0.046, are somewhat more sensitive in this respect.

IV. RESULTS

In this section, we present some results of the Dyson(1) and Dyson(2) calculations on the second-row atoms B, C, N, O, and F. These open-shell atoms show near-degeneracy effects in the valence-shell, and the presence of strongly interacting configurations[17] make a high-level treatment of electronic correlations mandatory. A comparison between theoretical results obtained in this work and with those obtained in other computational schemes available in the GAUSSIAN 98 package[18] (standard HF, post-HF, DFT) and experiment is performed. In the DFT calculations, two commonly used functionals were applied (BLYP and B3LYP), while the standard HF calculations are performed on the HF/6-311G** level. The post-HF methods include electron correlations by means of different perturbation schemes such as Møller–Plesset perturbation theory (MP2, MP4) or configuration interaction (CI). Throughout this paper, all results are denoted in atomic units.

First, we discuss some s.p. properties for the open-shell atoms. In Tables III and IV we report the prediction of the first ionization energies, respectively, the electron affinities. These properties can be calculated in two distinct ways. One method is the so-called adiabatic approach, where the atom and ion are optimized separately and the ground-state energies are subtracted subsequently. In this way, collective features such as relaxation of the orbitals are included and rearrangement effects in the mean field of the $(A\pm 1)$ system due to the removal or addition of an electron are taken into account. The present Green's function treatment, on the other hand, is a perturbative expansion starting from the neutral atom. The energy poles of the exact Green's function give simultaneously the excitation energies of the $(A\pm 1)$ electron system. This approach does not take rearrangement effects directly into account, as in the adiabatic scheme. The highest pole in the backward propagating part corresponds to the ionization energy which is in first order (HF approximation) represented by the HF s.p. energy of the highest occupied bound level.

We note that Koopmans' theorem is not valid for Kohn–Sham (KS) levels as clearly demonstrated by the poor DFT results (see third and fourth numerical column of Table III). On the other hand, the adiabatic DFT results (first two columns in Table III) show a remarkable agreement with experiment, which emphasizes the semiempirical nature of the DFT-functionals and the inclusion of these atoms in the training set. The nonadiabatic HF estimates are reasonable, indicating that Koopmans' theorem is valid in HF approximation to some extent, but apparently insufficient correlations are involved to get a more stringent agreement. Anyway, Dyson(1) provides a good starting point for Dyson(2) and it is obvious that the correlations included in the self-consistent second-order scheme generally have a beneficial effect. To

TABLE III. First ionization energies (in atomic units). Dyson(1) stands for Hartree–Fock in the discrete basis discussed in the text. Dyson(2) gives the solution of the second order Dyson equation after one and two iterations, and after convergence. In the first two numerical columns the adiabatic approach is used. In the next seven columns s.p. energies are used.

	DFT				HF		Dyson(2)			
	$E_{0(A)}-E_{0(A-1)}$		$-\epsilon_\alpha^{\mathrm{KS}}$		$-\epsilon_\alpha^{\mathrm{HF}}$		$-\epsilon_\alpha^{b}$			
	BLYP	B3LYP	BLYP	B3LYP	HF/6-311G**	Dyson(1)	First it.	Second it.	Conv.	Expt.
B	0.316	0.321	0.143	0.187	0.317	0.311	0.308	0.304	0.305	0.3050[a]
C	0.417	0.424	0.211	0.264	0.437	0.435	0.417	0.415	0.415	0.41381[b]
N	0.532	0.538	0.286	0.352	0.568	0.571	0.534	0.535	0.537	0.53412[c]
O	0.514	0.516	0.256	0.324	0.516	0.510	0.480	0.483	0.484	0.50046[d]
F	0.643	0.647	0.353	0.431	0.673	0.674	0.608	0.616	0.619	0.64028[e]

[a]Reference 19.
[b]Reference 20.
[c]Reference 21.
[d]Reference 22.
[e]Reference 23.

illustrate the convergence to self-consistency, results of the first and second iteration are given as well. It is observed that Dyson(1) overestimates the ionization energy for all open-shell atoms in this study and that the evolution toward convergence in Dyson(2) is mostly monotonous.

In Table IV we collected the results for the electron affinity, which is known as one of the atomic properties that are hardest to reproduce in an *ab initio* calculation. The electron affinity provides a useful test of the computational method because correlations are generally believed to be extremely important. This holds in particular for boron which forms the most weakly bound stable ion among the light elements,[24] and has been the subject of many theoretical studies.[28–33] Also the existence of the negative ion of nitrogen has a long history: from the early experiment of Fogel' *et al.*[34] and the dissociative attachment experiment of Hotop *et al.*[35] up until now, no proof of the existence of this ion has been published. Computational estimates vary as well.[36,37] The last two atoms (O and F) are known to have electron affinities that are of the most difficult ones to reproduce (see, e.g., Refs. 27,30,31,38).

The fact that electron correlations play a dominant role in the electron affinity is clearly demonstrated by the HF results [Dyson(1)], which fail in reproducing even the qualitative trend of the binding energies of the $(A+1)$ system vs A-particle system, resulting into a negative affinity (i.e., no electron can be bound). The first two columns of Table IV give the electron affinities as obtained in DFT calculations using standard functionals. We also report coupled-cluster calculations (CCSDT) with inclusion of various correction terms;[27] their predicted theoretical values are the best available in literature and are defined following an adiabatic approach, $E_0(A)-E_0(A+1)$. Very large basis sets are used and various corrections such as extrapolation to the basis-set limit and relativistic effects have been considered. As a consequence, the results of Ref. 27 have an excellent agreement with experiment but they are not completely self-consistent and not free from any empirical input.

To demonstrate the fact that correlations (as implemented in DFT) are extremely important to reproduce a sensitive observable such as the electron affinity we also include in Table IV adiabatic HF results using finite basis sets (HF/6-311G**). They are scarcely better than the Dyson(1) results, i.e., the lowest unoccupied HF s.p. energies in the discretized basis. No extra electron can be bound in the HF system (apart from the highly electronegative F), and we conclude that both HF schemes completely fail in reproducing even the qualitative trend of the electron affinity throughout the second-row atomic systems.

As opposed to HF, the Dyson(2) results turn out to be quite satisfactory. For most atoms the first iteration yields a drastic change in the right sense, but the predicted values for the electron affinity still vary significantly from the converged values. This supports the important role of the com-

TABLE IV. Electron affinities (in atomic units). See also caption of Table III. In the first four numerical columns the adiabatic approach is used. In the next four columns s.p. energies are used.

	DFT		CCSDT	HF		Dyson(2)			
	$E_{0(A)}-E_{0(A+1)}$			$-\epsilon_a^{\mathrm{HF}}$		$-\epsilon_a^{f}$			
	BLYP	B3LYP	Ref. 27	HF/6-311G**	Dyson(1)	First it.	Second it.	Conv.	Expt.
B	−0.0165	−0.0102	0.01024	−0.030	−0.0358	−0.003	0.006	0.008	0.010279(64)[a]
C	0.0145	0.0202	0.04641	−0.002	−0.0198	0.033	0.045	0.046	0.046382(0)[b]
N	−0.0470	−0.0438	-	−0.109	−0.1080	−0.0491	−0.039	−0.039	<0
O	0.0012	0.0057	0.05368	−0.060	−0.0792	0.014	0.032	0.032	0.053695(3)[c]
F	0.0642	0.0675	0.12505	0.006	−0.0369	0.098	0.126	0.126	0.124991(5)[c]

[a]Reference 24.
[b]Reference 25.
[c]Reference 26.

TABLE V. Single-particle properties (energies in atomic units). Experimental data for core levels from Ref. 40; for the valence levels, see Table III.

		Single-particle energies					Spectr. strength
		HF/6-311G**	HF([a])	Dyson(1)	Dyson(2)	Expt.	Dyson(2)
B	$1s\downarrow$	−7.697		−7.702	−7.471		0.839
		−7.695			−6.91		
	$1s\uparrow$	−7.682		−7.687	−7.451		0.845
	$2s\downarrow$	−0.543		−0.543	−0.524		0.900
		−0.495					
	$2s\uparrow$	−0.444		−0.445	−0.457		0.932
	$2p\downarrow$	−0.317	−0.310	−0.311	−0.305	−0.3050	0.952
C	$1s\downarrow$	−11.34		−11.35	−11.00		0.811
		−11.33			−10.44		
	$1s\uparrow$	−11.30		−11.30	−10.94		0.819
	$2s\downarrow$	−0.826		−0.827	−0.755		0.847
		−0.706					
	$2s\uparrow$	−0.582		−0.582	−0.591		0.926
	$2p\downarrow$	−0.437	−0.433	−0.435	−0.415	−0.41381	0.942
N	$1s\downarrow$	−15.67		−15.67	−15.25		0.850
		−15.63			−15.06		
	$1s\uparrow$	−15.57		−15.58	−15.19		0.866
	$2s\downarrow$	−1.160		−1.163	−1.023		0.814
		−0.945					
	$2s\uparrow$	−0.724		−0.725	−0.731		0.928
	$2p\downarrow$	−0.568	−0.568	−0.571	−0.537	−0.53412	0.938
O	$1s\downarrow$	−20.70		−20.71	−19.89		0.586
		−20.67			−19.96		
	$1s\uparrow$	−20.62		−20.63	−19.90		0.721
	$2s\downarrow$	−1.410		−1.418	−1.253		0.827
		−1.244					
	$2s\uparrow$	−1.070		−1.073	−1.025		0.908
	$2p\downarrow$	−0.703/−0.606		−0.693/−0.649	−0.632/−0.589		0.918/0.909
		−0.632					
	$2p\uparrow$	−0.516		−0.510	−0.484	−0.50046	0.930
F	$1s\downarrow$	−26.40		−26.41	−25.78		0.852
		−26.38			−25.60		
	$1s\uparrow$	−26.35		−26.36	−25.79		0.848
	$2s\downarrow$	−1.663		−1.672	−1.498		0.857
		−1.573					
	$2s\uparrow$	−1.469		−1.474	−1.367		0.894
	$2p\downarrow$	−0.834/−0.724		−0.803/−0.752	−0.723/−0.677		0.909/0.905
		−0.730					
	$2p\uparrow$	−0.673		−0.674	−0.619	−0.64028	0.916

[a]Reference 32.

plex electron correlations generated through the ''dressed'' second-order self-energy. For boron it is noted that the second iteration is even required for binding an additional particle. For the nitrogen atom the electron affinity remains negative, in agreement with experiment where no stable negative nitrogen ion can be found. Of course the present calculation, being nonvariational in nature, cannot rule out the existence of a stable negative nitrogen ion. Moreover, for such a system at the edge of stability the description of the single-particle continuum is likely to be crucial. Nevertheless, all atoms start from the same type of HF spectrum, having no bound unoccupied *p*-orbital, and it is satisfactory to see that the electron correlations in the Dyson(2) scheme pull down one *p*-orbital to negative energies for all atoms in Table IV, except for nitrogen.

The final converged Dyson(2) results show good agreement with the experimental trend, and for carbon and fluor the predicted electron affinity is even remarkably accurate. In this respect one should emphasize that the electron affinity derived in the Dyson(2) scheme represents a pole in the spectral representation of the neutral atom Green's function, which simultaneously contains information on electron affinities and ionization energies. The electron affinity is not determined from separate calculations of the ground-state energies of neutral atom and negative ion.

A summary of all s.p. energies is given in Table V. The energies in the first numerical column are standard HF results obtained in finite basis sets using the GAUSSIAN 98 software package. The second column collects the HF energies from a computational scheme that also solves the HF equations in coordinate space.[39] This scheme solves the single-configuration HF equations, without distinguishing spins. Fi-

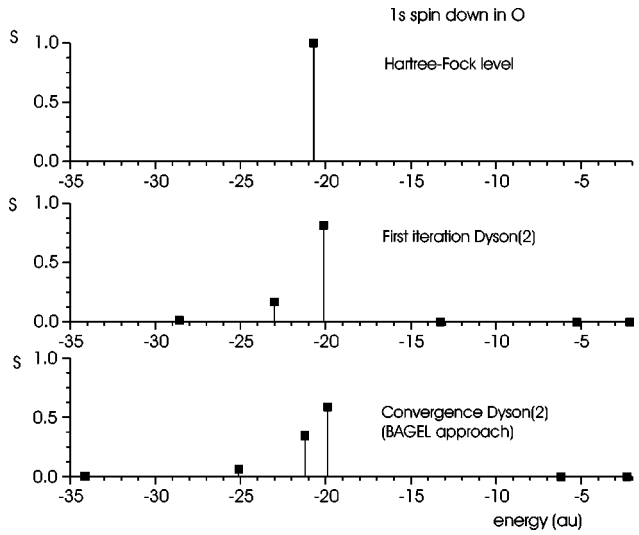

FIG. 2. Spectroscopic factor of $1s\downarrow$ in O as predicted in the Dyson(1) and Dyson(2) scheme.

nally the energies of both Dyson(1) and Dyson(2) schemes are reported in the next two columns. A thorough discussion has already been held for the valence ionization energies. For the core levels the experimental information is less accurate; experiments on open-shell atoms are more involved than for the closed-shells atoms and are generally limited to a rather narrow energy range. Therefore the experimental data in Table V are deduced from experiments on solids. Since these levels are so tightly bound that they are relatively inert, we assume that their energies are more or less independent of the state of aggregation. The predictions for the core s.p. energies in the two HF schemes [HF/6-311G** and Dyson(1)] are similar, which is not surprising as a correct treatment of the configuration space will mainly affect s.p. levels around the Fermi surface. The Dyson(2) scheme seems to make the core levels somewhat less bound in agreement with experiment.

In Fig. 2 we demonstrate the fragmentation process of the 1s level of oxygen from Dyson(1) to the converged Dyson(2) result. It is noted that the first iteration in the second-order procedure scatters the spectroscopic strength over a large energy range and that the correlations induce a shift of the quasiparticle energy (i.e., the energy of the largest peak) towards the Fermi energy. The effect of self-consistency is mainly to regroup the strength into a few fragments and to further deplete the quasiparticle peak, while its energy varies only little.

Table VI gives an overview of various predictions of the total ground-state energy of the open-shell systems.

The DFT results are superior to those of the other schemes: it was already mentioned in the paper of Becke[42] that the correction of the BLYP functional,[43] determined by a least-squares fit to the noble-gas atoms helium through radon, also gives an excellent prediction of the binding energies in the light open-shell systems present in this study. On the other hand, the B3LYP functional,[44] an extension of the BLYP functional, has been determined by fitting its parameters a.o. to the total binding energies of B, C, N, O, and F. Therefore we would expect an even better agreement with experiment for this functional. However, due to the larger training set of B3LYP compared to BLYP, some slightly larger deviations appear for the former. We include three HF calculations in Table VI. Their results are almost identical, though Dyson(1) unsurprisingly predicts a somewhat larger binding energy, since it stands for the exact HF solution in coordinate space. The other two schemes either suffer from finite basis effects (HF/6-311G**) or do not adopt the spin degree of freedom in the calculation (Ref. 39) which leads to a slightly less bound system.

We also include in Table VI some post-HF results based upon application of perturbation techniques beyond HF, such as MP2, MP3 and a few MP4 schemes. Finally a variational calculation (configuration interaction or CI) has been performed. When comparing these results with the Dyson(2) energies it should be kept in mind that the post-HF results were all performed using standard finite basis sets, which

TABLE VI. Total ground-state energy (atomic units) obtained with various many-body models. In MP4, calculations with double-quadruple (DQ), single-double-quadruple (SDQ), and single-double-triple-quadruple (SDTQ) substitutions in the ground-state Slater determinant are considered. Experimental data are from Ref. 41.

		B	C	N	O	F
DFT	DFT-BLYP	−24.649	−37.842	−54.583	−75.073	−99.742
	DFT-B3LYP	−24.662	−37.856	-54.599	-75.085	-99.754
HF	HF/6-311G**	−24.530	−37.689	−54.398	−74.805	−99.397
	HF[a]	−24.529	−37.689	−54.401	−74.809	−99.409
	Dyson(1)	−24.530	−37.690	−54.405	−74.815	−99.412
Post-HF	MP2	−24.569	−37.745	−54.475	−74.918	−99.554
	MP3	−24.583	−37.760	−54.488	−74.931	−99.563
	MP4(DQ)	−24.588	−37.764	−54.490	−74.932	−99.563
	MP4(SDQ)	−24.588	−37.764	−54.490	−74.932	−99.564
	MP4(SDTQ)	−24.588	−37.764	−54.491	−74.933	−99.565
CI	QCISD	−24.591	−37.766	−54.491	−74.933	−99.564
Dyson(2)	First it.	−24.585	−37.766	−54.505	−74.944	−99.565
	Second it.	−24.597	−37.786	−54.542	−75.008	−99.676
	Conv.	−24.600	−37.789	−54.543	−75.010	−99.678
Expt.		−24.653	−37.844	−54.587	−75.063	−99.725

[a]Reference 39.

makes a quantitative comparison with Dyson(2) somewhat unfair. They are merely given to get an idea about the effect of gradually including a larger amount of correlations in the description. All these calculations predict binding energies that are larger and closer to the experimental outcome compared to HF. However, the electron correlations in these perturbation models are not of the same complexity as those present in the Dyson(2) scheme.

V. SUMMARY AND CONCLUSIONS

In this paper, our computational scheme to solve Dyson's equation up to second order has been extended to open-shell systems. The overall algorithm as developed for closed-shell systems in Ref. 1 is maintained, apart from some slight adjustments. The first part of the scheme consists in solving the Hartree–Fock equations in coordinate space. To allow a numerical description of the continuum, a confining potential wall is added. The resulting discrete basis set is truncated in such a way that it offers a good description of the continuum and that it is complete for all practical purposes. Since the electrons in the system no longer couple to zero total angular momentum and the equations are solved in the uncoupled representation, a more involved set of quantum numbers is required. The labeling scheme can however be simplified by means of angular averaging of the spin–orbitals. As in the closed-shell case, the BAGEL approach is adopted to cope with the huge increase in the number of poles over the iterations in the second-order scheme.

The method is applied to the open-shell atoms B, C, N, O, and F and comparison is made with experiment and other computational tools on the levels of Hartree–Fock, post-Hartree–Fock, configuration interaction and Density Functional Theory. Special attention is devoted to the reproduction of the ionization energy, the electron affinity, single-particle energies and total binding energy. The Dyson(2) scheme produces substantial shifts from the Hartree–Fock estimates and brings the theoretical prediction closer to experiment. Especially the electron affinity is a testing observable for the scheme because correlation effects play a dominant role in this property. The Dyson(2) scheme performs fairly well in predicting this quantity, especially in the case of fluor. It also confirms the experimentally predicted instability of the anion of nitrogen.

The key advantage of the Green's function formalism is that the nature of the included correlations can be identified by means of Feynman diagrams as was discussed thoroughly in our previous paper. Therefore, we intend to use the Dyson(2) calculations to learn more about the correlations which are implemented in functionals for DFT. In this respect, the extension to open-shell systems is important to gain insight in to the spin dependent correlations. The microscopic approach presented in this and the previous work can be employed to identify a ''universal background'' contribution to correlation effects in atomic and molecular systems. In this way Green's function calculations can shed new light on the correlations which are (to be) included in exchange-correlation functionals for use in DFT.

ACKNOWLEDGMENT

This work was supported by the Fund for Scientific Research-Flanders (FWO).

[1] D. Van Neck, K. Peirs, and M. Waroquier, J. Chem. Phys. **115**, 15 (2001).
[2] J. Linderberg and Y. Öhrn, *Propagators in Quantum Chemistry* (Academic, London, 1973)
[3] Y. Öhrn, *The World of Quantum Chemistry*, edited by B. Pullman and R. Parr (Reidel, Dordrecht, 1976), p. 57.
[4] L. S. Cederbaum and W. Domcke, Adv. Chem. Phys. **36**, 205 (1977).
[5] G. Csanak, H. S. Taylor, and R. Yaris, in *Advances in Atomic and Molecular Physics*, edited by D. R. Bates and I. Esterman (Academic, New York, 1971), Vol. 7, p. 287.
[6] W. von Niessen, G. H. F. Diercksen, and L. S. Cederbaum, J. Chem. Phys. **67**, 4124 (1977).
[7] M. F. Herman, K. F. Freed, and D. L. Yeager, in *Advances in Chemical Physics*, edited by I. Prigogine and S. A. Rice (Wiley, New York, 1981), Vol. 48.
[8] J. Simons, J. Chem. Phys. **55**, 1218 (1971).
[9] J. D. Doll and W. P. Reinhardt, J. Chem. Phys. **57**, 1169 (1972).
[10] J. Simons, J. Chem. Phys. **59**, 1218 (1973).
[11] H. Müther, T. Taigel, and T. T. S. Kuo, Nucl. Phys. A **482**, 601 (1988).
[12] H. Müther and L. D. Skouras, Nucl. Phys. A **555**, 541 (1993).
[13] H. Müther and L. D. Skouras, Phys. Lett. B **306**, 201 (1993).
[14] H. Müther and L. D. Skouras, Nucl. Phys. A **581**, 247 (1995).
[15] Y. Dewulf, D. Van Neck, L. Van Daele, and M. Waroquier, Phys. Lett. B **396**, 7 (1997).
[16] G. H. Golub and C. H. Van Loan, *Matrix Computations* (Johns Hopkins University Press, Baltimore, 1996).
[17] M. J. Vilkas, Y. Ishikawa, and K. Koc, Phys. Rev. A **60**, 2808 (1999).
[18] GAUSSIAN 98, Revision A.7, M. J. Frisch, G. W. Trucks, H. B. Schlegel *et al.*, Gaussian, Inc., Pittsburgh, Pennsylvania, 1998.
[19] C. M. Brown, S. G. Tilford, and M. L. Ginter, J. Opt. Soc. Am. **64**, 877 (1974).
[20] L. Johansson, Ark. Fys. **31**, 201 (1966).
[21] K. B. S. Eriksson and J. E. Pettersson, Phys. Scr. **3**, 211 (1971).
[22] K. B. S. Eriksson and H. B. S. Isberg, Ark. Fys. **37**, 221 (1968).
[23] B. Edlén, Sol. Phys. **9**, 439 (1969).
[24] M. Scheer, R. C. Bilodeau, and H. K. Haugen, Phys. Rev. Lett. **80**, 2562 (1998).
[25] M. Scheer, R. C. Bilodeau, C. A. Brodie, and H. K. Haugen, Phys. Rev. A **58**, 2844 (1998).
[26] *CRC Handbook of Chemistry and Physics*, 78th ed. (CRC, Boca Raton, 1997).
[27] G. de Oliveira, J. M. L. Martin, F. de Proft, and P. Geerlings, Phys. Rev. A **60**, 1034 (1999).
[28] K. Raghavachari, J. Chem. Phys. **82**, 53 (1985).
[29] D. Sundholm and J. Olsen, Chem. Phys. Lett. **171**, 53 (1990).
[30] T. Noro, M. Yoshimine, M. Sekiya, and F. Sasaki, Phys. Rev. Lett. **66**, 1157 (1991).
[31] R. A. Kendall, T. H. Dunning, Jr., and R. J. Harrison, J. Chem. Phys. **96**, 6796 (1992).
[32] C. Froese-Fischer, A. Ynnerman, and G. Gaigalas, Phys. Rev. A **51**, 4611 (1995).
[33] W. P. Wijesundera, Phys. Rev. A **55**, 1785 (1997).
[34] Ya. M. Fogel', V. F. Kozlov, and A. A. Kalmykov, Zh. Éksp. Teor. Fiz. **36**, 1354 (1959) [Sov. Phys. JETP **9**, 963 (1959)].
[35] H. Hotop and W. J. Lineberger, J. Phys. Chem. Ref. Data **14**, 731 (1985).
[36] B. Hird and S. P. Ali, Phys. Rev. Lett. **41**, 540 (1978).
[37] W. P. Wijesundera and F. A. Parpia, Phys. Rev. A **57**, 3462 (1998).
[38] R. J. Gdanitz, J. Chem. Phys. **110**, 706 (1999).
[39] C. Froese Fischer, *The Hartree–Fock Method for Atoms: A Numerical Approach* (Wiley, New York, 1977).
[40] *Photoemission in Solids I: General Principles*, with additional corrections, edited by M. Cardona and L. Ley (Springer-Verlag, Berlin, 1978).
[41] A. Veillard and E. Clementi, J. Chem. Phys. **49**, 2419 (1968).
[42] A. D. Becke, Phys. Rev. A **38**, 3098 (1988).
[43] C. Lee, W. Yang, and R. G. Parr, Phys. Rev. B **37**, 785 (1988).
[44] A. D. Becke, J. Chem. Phys. **98**, 5648 (1993).